Chinese Chemical Letters 35 (2024) 108913

Contents lists available at ScienceDirect

Chinese Chemical Letters

journal homepage: www.elsevier.com/locate/cclet

A mitochondria-targeted H_2S-activatable fluorogenic probe for tracking hepatic ischemia-reperfusion injury

Bin Fang[a,b,1], Jiaqi Yang[b,1], Limin Wang[b,1], Haoqin Li[b], Jiaying Guo[b], Jiaxin Zhang[b], Qingyuan Guo[b], Bo Peng[b,c,e], Kedi Liu[f], Miaomiao Xi[f], Hua Bai[b,c,*], Li Fu[a,*], Lin Li[b,d,e,*]

[a] School of Materials Science and Engineering, Northwestern Polytechnical University, Xi'an 710072, China
[b] Frontiers Science Center for Flexible Electronics, Xi'an Institute of Flexible Electronics (IFE) and Xi'an Institute of Biomedical Materials & Engineering, Northwestern Polytechnical University, Xi'an 710072, China
[c] Key laboratory of Flexible Electronics of Zhejiang Province, Ningbo Institute of Northwestern Polytechnical University, Ningbo 315103, China
[d] The Institute of Flexible Electronics (IFE, Future Technologies), Xiamen University, Xiamen 361005, China
[e] Wuhan National Laboratory for Optoelectronics - Advanced Biomedical Imaging Facility, Huazhong University of Science and Technology, Wuhan 430074, China
[f] TANK Medicinal Biology Institute of Xi'an, Xi'an 710032, China

ARTICLE INFO

Article history:
Received 25 June 2023
Revised 5 August 2023
Accepted 7 August 2023
Available online 9 August 2023

Keywords:
Mitochondria-targeted
Bioimaging
H_2S-activatable
Fluorogenic probe
Hepatic ischemia-reperfusion injury (HIRI)

ABSTRACT

Hepatic ischemia-reperfusion injury (HIRI) is the cause of postoperative hepatic dysfunction and failure, and even death. As an important biological effector molecule, hydrogen sulfide (H_2S) of mitochondria as a gasotransmitter that is usually used to protect against acute HIRI injury. However, the exact relationship between HIRI and mitochondrial H_2S remains tangled due to the lack of an effective analytical method. Herein, we have fabricated a mitochondria-targeted H_2S-activatable fluorogenic probe (Mito-GW) to explore the stability of mitochondrial H_2S and track the changes of mitochondrial H_2S during the HIRI. By virtue of pyridinium electropositivity and its amphiphilicity, Mito-GW could accumulate in mitochondria. It goes through an analyte-prompted immolation when reacts with H_2S, resulting in the releasing of the fluorophore (GW). Therefore, the extent of Mito-GW conversion to GW can be used to evaluate the changes of mitochondrial H_2S level in living cells and tissues. As proof-of-principle, we have used Mito-GW to demonstrate the mitochondria H_2S-levels increase and then decrease during HIRI *in vitro* and *in vivo*. Our research highlights the tremendous potential of Mito-GW as a mitochondrial H_2S fluorogenic probe in elucidating the pathogenesis of HIRI, providing a powerful tool for promoting future research on hepatology.

As a common clinical complication, hepatic ischemia reperfusion injury (HIRI) is arising from a range of situations such as hepatectomy and transplantation surgery [1–3]. The process of HIRI can lead to severe liver malfunction, ultimately leading to graft rejection, liver failure, or even death in liver transplant patients [4–6]. Under different pathological conditions, HIRI can be classified into cold and warm HIRI due to ambient temperature [7–9]. It is well known that HIRI involves multiple mechanisms, including mitochondrial dysfunction [10], anaerobic metabolism [11], ROS overproduction [12–14], pH imbalance [15], calcium overload [16], *etc*. Despite significant improvements in perioperative care and surgical techniques, therapeutic strategies to inhibit bedside HIRI remain hampered, mainly attributing to the complex mechanisms underlying the process [7]. In a fact, abnormalities at the molecular-level occur prior to those at the histological-level during the HIRI process. If HIRI can be clearly identified at an early stage, it will be convenient for us to use effective means of prevention and treatment to minimize HIRI. Therefore, detection of molecular-level changes in chemical species during the HIRI is crucial for avoiding HIRI and thus saving patients.

Hydrogen sulfide (H_2S), as a gasotransmitter, has gained considerable attention due to its crucial role in participating in various physiological and pathological processes including inflammation, mitochondrial functions and cell survival [17–19]. H_2S is produced primarily in the mitochondria by cystathionine-γ-lyase (CSE) and

* Corresponding authors.
E-mail addresses: iamhbai@nwpu.edu.cn (H. Bai), fuli@nwpu.edu.cn (L. Fu), ifelli@xmu.edu.cn (L. Li).
[1] These authors contributed equally to this work.

https://doi.org/10.1016/j.cclet.2023.108913
1001-8417/

3-mercaptopyruvate sulfurtransferase (3-MST). Studies have shown that low concentrations of mitochondrial H_2S can enhance hepatic mitochondrial electron transport and cellular bioenergetics to some extent, while conversely it inhibits cellular bioenergetics [20,21]. Meanwhile, H_2S can protect mitochondria from HIRI by reducing oxidative stress and improving energy metabolism, thus it plays a pivotal role in controlling mitochondrial functions and cell survival of the liver [22,23]. However, the relationship between H_2S and HIRI remains tangled due to the lack of a useful analytical method. Therefore, in order to gain a deeper understanding of the level fluctuations of H_2S in HIRI, constructing a detection tool for mitochondrial H_2S is urgent.

As a non-invasive method, optical imaging has become widely used in monitoring real-time cellular bioactive analytes [24–28] and studying the cellular micro-environment (including viscosity [29], temperature [30], polarity [31] and pH [32]) due to its simplicity of operation, real-time non-invasive imaging, high resolution, high sensitivity and good selectivity. In particular, small molecule-based fluorogenic probes (SMFPs) have demonstrated excellent performance, such as rapid excretion capacity, low toxicity in living organisms and ease of structural modification [33]. Therefore, many researchers have developed various SMFPs for evaluating molecular events in cells and *in vivo* [34,35]. Although many reports on fluorogenic probes being used to detect mitochondrial H_2S (Fig. S1 and Table S1 in Supporting information), there are remain some unresolved issues, such as low sensitivity, relatively high-background, poor solubility and inevitable biological toxicity. In addition, to our knowledge, there have been no reports of fluorogenic detection of mitochondrial H_2S in HIRI yet. Therefore, to reveal the mitochondrial H_2S-mediated HIRI, it is important to develop effective SMFPs and establish real-time imaging methods for monitoring H_2S levels and distribution.

Fluorophore with torsional intramolecular charge transfer (TICT) properties, usually have a "D-π-A" molecular configuration with electron-withdrawing unit (acceptor, A) and electron-donating unit (donor, D), its emission of the zero vibrational energy level is forbidden when in the TICT state and thus have negligible fluorescence emission and low background fluorescence signal, which facilitates the design of fluorogenic probe with high sensitivity [36,37]. Herein, we fabricated a novel naphthalene-based and self-immolative D-π-A fluorogenic probe (Mito-GW) triggered by mitochondrial H_2S for performing imaging and tracking changes of H_2S in HIRI. The probe comprises an H_2S-specific reduction reaction aryl azide moiety [36,38,39] coupled to the electron-withdrawing pyridinium cation which as a mitochondrial-targeting moiety due to superior membrane permeability and realize the mitochondrial H_2S monitor in HIRI. The naphthylamine fluorophore as a strong electron-donating moiety is incorporated into the designing of the probe. Donor and acceptor subunits are communicated in the probe through the conjugated π-bridge to form TICT effects. The probe is almost fluorescence silent owing to TICT properties [40–42], once reacting with mitochondrial H_2S, releasing fluorophore (GW) with strong fluorescence due to the cleavage leaves aryl azide moiety through self-immolation (Scheme 1). The probe has been utilized in detecting and assessing the changes of mitochondrial H_2S during the HIRI process.

The probe (Mito-GW) was constructed through Knoevenagel condensation of G2 and W3 (Scheme S1 in Supporting information). W3 can be easily obtained by the Suzuki reaction of 5-formyl-2-thiopheneboronic acid pinacol ester and W2. The molecular structures of the fluorogenic probe Mito-GW and other related intermediate products in the experiment were fully characterized by liquid chromatograph mass spectrometer (LC-MS), ^{1}H-nuclear magnetic resonance (^{1}H NMR) and ^{13}C NMR in Supporting information.

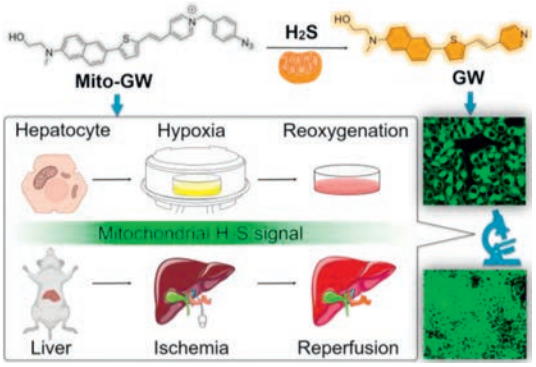

Scheme 1. Schematic representation for fabrication of a mitochondria-targeted H_2S-activatable fluorogenic probe for tracking hepatic ischemia-reperfusion injury *in vitro* and *in vivo*.

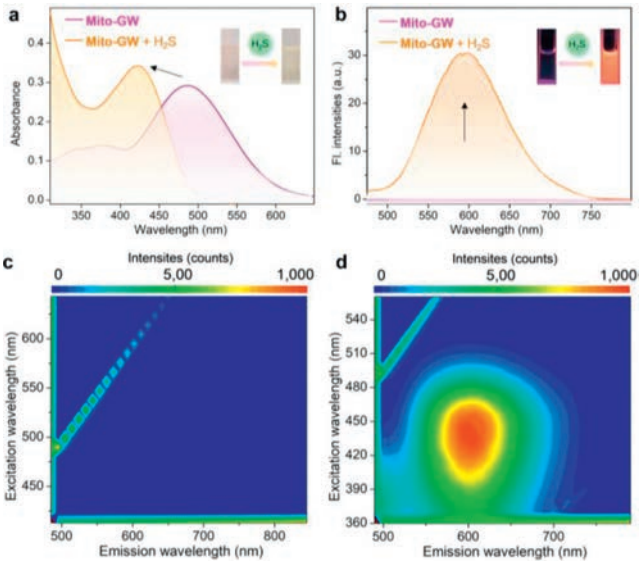

Fig. 1. (a) The ultraviolet–visible spectroscopy (UV–vis) absorption spectra of Mito-GW with or without H_2S in PBS buffer solution (10 mmol/L PBS; pH 7.42; containing 0.5% DMSO). Inset: the color changes of the fluorogenic probe and its reaction with H_2S through naked eyes. (b) The fluorescence responses of Mito-GW in the absence or presence of H_2S. Inset: the color changes of the fluorogenic probe and it reacting with H_2S by using a portable ultraviolet lamp with a wavelength of 365 nm. The excitation-emission mapping spectra of the Mito-GW (c) and Mito-GW + H_2S (d). Mito-GW: 10 μmol/L; H_2S: 100 μmol/L.

To verify whether our fluorogenic probe can selectively toward mitochondrial H_2S, we first investigated the optical characteristics of Mito-GW for H_2S. The absorption and emission spectra of the fluorogenic probe were measured with or without H_2S in phosphate buffer saline (PBS, pH 7.42) solution. As shown in Fig 1a, the maximum absorption of Mito-GW itself was 486 nm, and as H_2S was introduced into the probe solution, its absorption peak gradually blue-shift to 424 nm. It is important to note that the fluorogenic probe was initially non-fluorescence (Fig. 1c), which is due to the strong TICT effect. For low-background or background-free of a fluorogenic probe, it will be very beneficial for imaging and detecting bioactive molecules in organisms. Once NaHS, as the H_2S source, was interacted with the Mito-GW, there is a high contrast fluorescence signal enhancement phenomenon at 602 nm (Figs. 1b and d)), accompanied a strong orange red fluorescence enhancement phenomenon, observed by a 365 nm handheld ultraviolet lamp (insert). In addition, the fluorogenic probe had a large Stocks shift (178 nm). Therefore, Mito-GW could minimize the im-

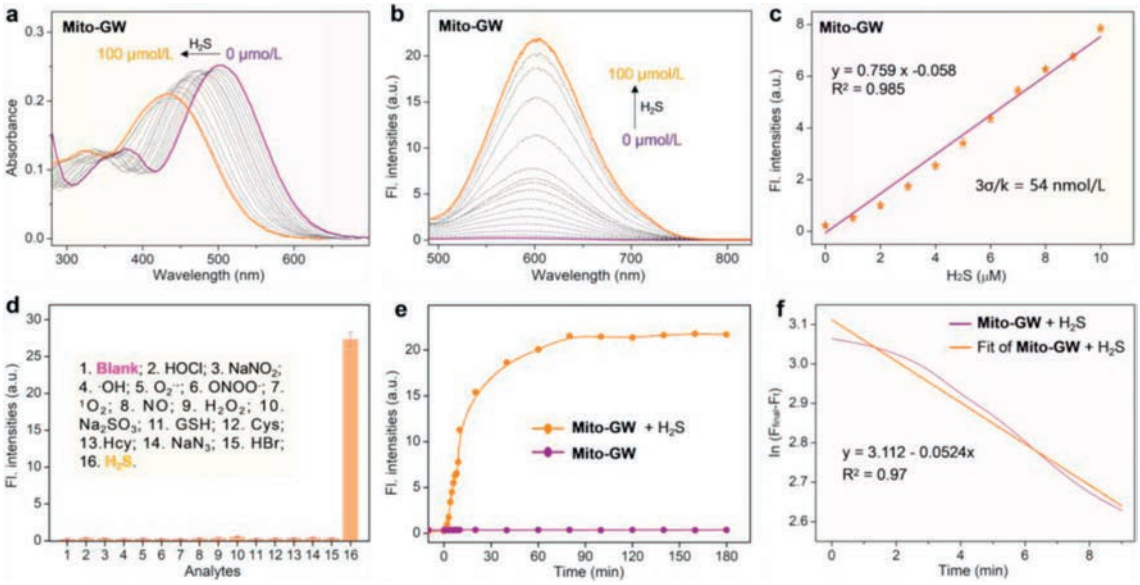

Fig. 2. (a) The absorbance spectra of Mito-GW (10 μmol/L) upon various concentrations of H_2S titration in PBS buffer solution (10 mmol/L PBS; pH 7.42; containing 0.5% DMSO). (b) The fluorescence response of Mito-GW upon on H_2S titration in PBS solution. (c) The plot of the fluorescence emission intensities at 602 nm against H_2S concentration. (d) The fluorescence emission intensities responses of Mito-GW with various analytes in PBS solution: 1. Blank, 2. ClO^-, 3. NO_2^-, 4. $^{\bullet}OH$, 5. $O_2^{\bullet-}$, 6. $ONOO^-$, 7. $^1O_2$, 8. NO, 9. H_2O_2, 10. SO_3^{2-}, 11. GSH, 12. Cys, 13. Hcy, 14. N_3^-, 15. Br^-, 16. H_2S. $\lambda_{em} = 602$ nm. These values were the mean ± standard deviation (SD). (e) The reaction kinetics of Mito-GW (10 μmol/L) was tested *via* recording the time-dependent fluorescence emission intensities of the fluorogenic probe at 602 nm to H_2S (100 μmol/L H_2S). (f) The reaction rate constant of the fluorogenic probe toward H_2S was to be $k_{obs} = 5.2 \times 10^{-2}$ min^{-1} by calculating its pseudo first order kinetics.

pact of molecular self-absorption when detecting and evaluating the level of H_2S in living cells.

The above experimental results fully validate our design purpose, which is that the probe had the potential to achieve quantitative analysis and detection of H_2S. Therefore, it inspired us to further explore the sensitivity of the probe to H_2S. The absorption (Fig. 2a and Fig. S5 in Supporting information) and emission spectra response (Fig. 2b) of Mito-GW to various concentrations of H_2S in PBS solution were tested. As shown in Fig. 2c, the fluorescence intensities of the fluorogenic probe exhibited dose-dependent emission enhancement with increasing concentration of H_2S range from 0 to 100 μmol/L. As H_2S is introduced into the probe system, as its concentration gradually increased, the fluorescence intensities of the probe significantly enhancement and exhibited a dose-dependent effect. After analysis (Fig. 2c), we found that there is a favorable linear relationship between the fluorescence emission intensities at 602 nm of the fluorogenic probe and the concentrations of H_2S, which was $y = -0.058 + 0.759$ $[H_2S]$ ($R^2 = 0.985$). Through further calculation, the detection limit of the fluorogenic probe for H_2S was to be 54.0 nmol/L (limit of detection, LOD, $3\sigma/k$). The above experimental results fully demonstrated that Mito-GW could be used as a useful detection method for quantitative evaluation the level of H_2S *in vitro*.

Next, we investigated the specific fluorescence response of Mito-GW to H_2S on various analytes widely existing in biological environments, including reactive nitrogen species (NO_2^-, $ONOO^-$ and NO), reactive sulfur species (SO_3^{2-}), reductant species (Br^- and N_3^-), biothiols (GSH, Hcy and Cys), and reactive oxygen species (ClO^-, $^{\bullet}OH$, H_2O_2, $O_2^{\bullet-}$ and $^1O_2$). As presented in Fig. 2d and Fig. S6 (Supporting information), the fluorescence of Mito-GW did not change for other species except HS^-, implying that Mito-GW can serve as an excellent fluorogenic probe with ultra-high selectivity for H_2S. In addition, we investigated the stability of Mito-GW under physiological conditions (Fig. S7 in Supporting information). The results indicated that Mito-GW can be used to recognize H_2S species under a wide range of pH 5.0 to 12.0, accompanied by significant fluorescence emission at 602 nm and stable fluorescence intensities. Subsequently, the reaction kinetics of Mito-GW was also investigated by recording the time-dependent fluorescence emission intensities of the fluorogenic probe at 602 nm to H_2S (Fig. 2e). Mito-GW interacted with H_2S and reacted almost completely within 45 min without any catalyst. The reaction rate constant of the fluorogenic probe toward H_2S was to be $k_{obs} = 5.2 \times 10^{-2}$ min^{-1} by calculating its pseudo first order kinetics (Fig. 2f). The above experimental results fully demonstrated that Mito-GW detection of H_2S with high sensitivity and specificity, and had the potential to detect the level fluctuations of H_2S during HIRI processes.

We continued to explore the reaction mechanism of the probe towards H_2S and proposed a possible reaction process as shown in Fig. 3a. The probe is non-fluorescence owe to the strong TICT effect. When H_2S species were introduced into the reaction, the aryl azide unit of Mito-GW would self-immolative cleaved, releasing a fluorophore GW with strong fluorescence emission due to the ICT effect. Next, the ground state structures of the probe Mito-GW and fluorophore GW (Fig. 3b), and their absorption spectra (Fig. 3c) were optimized using Gaussian 09. The electrostatic potential and molecular orbital energy of Mito-GW and GW were investigated by frontier molecular orbital (FMO) and density functional theory (DFT) to easy explain the mechanism of switch-on fluorescence response of the probe for H_2S (Fig. 3d and Table S2 in Supporting information). Since the electron-withdrawing ability of the pyridinyl moiety arise from the probe had changed significantly before and after reaction with H_2S, the excited state of fluorophore GW formed ICT state instead of TICT state, resulting in strong fluorescence emission. We carried out high performance liquid chromatography (HPLC) experiments to further verify our speculation on the mechanism of Mito-GW toward H_2S (Fig. 3e). Once Mito-GW reacted with H_2S, its signal gradually disappeared, followed by the emergence of two new peaks corresponding to Mito-G and GW, which were fully confirmed through further analysis from mass spectrometry (MS) (Figs. S8 and S9 in Supporting in-

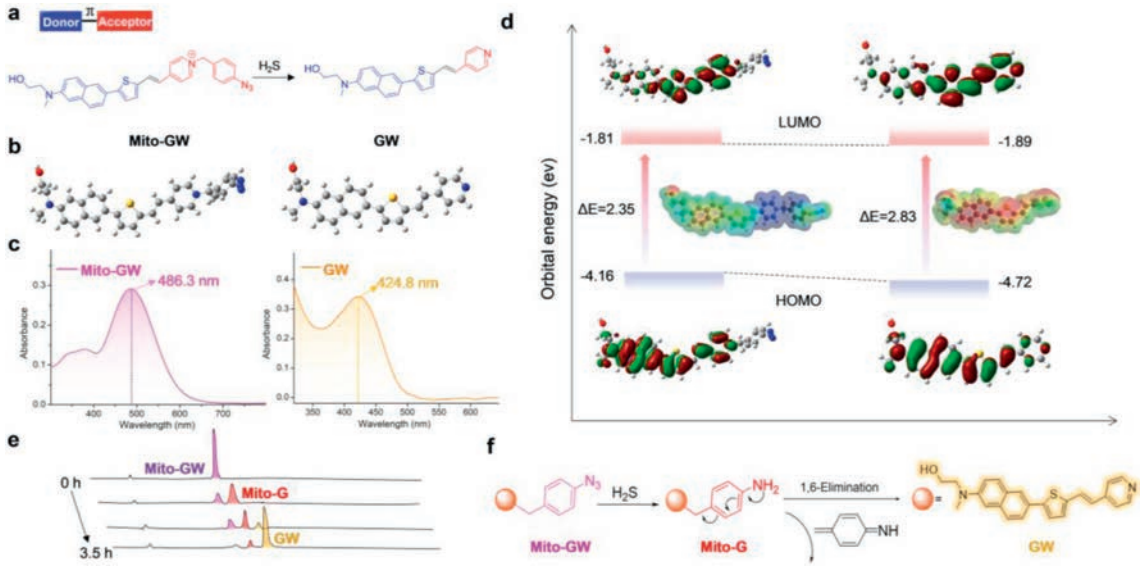

Fig. 3. (a) The molecular structures of fluorogenic probe Mito-GW and fluorophore GW. (b) The DFT optimized ground state geometric structures of fluorogenic probe and fluorophore. The structures of the molecules were represented by ball-and-stick, nitrogen, carbon, hydrogen, boron and oxygen atoms are colored in blue, gray white, pink and red, respectively. (c) The absorption spectra of fluorogenic probe and fluorophore. (d) The frontier molecular orbitals of fluorogenic probe and fluorophore were calculated by DFT. Highest occupied molecular orbital (HOMOs), ground states; Lowest unoccupied molecular orbital (LUMOs), excited states; the electrostatic potential (ESP) maps were plotted with the color range from blue [3.6 electron, positive] to red [−4.15 electron, negative]. (e) The HPLC traces of Mito-GW after 3.5 h incubation in H_2S solution at 37 °C (pH 7.42). (f) The proposed reaction mechanism for Mito-GW toward H_2S.

formation). The new peaks appearing at $m/z = 387.24$ ($[M+H]^+$) and $m/z = 246.76$ ($[M]^+/2$) corresponding to GW and Mito-G, respectively. The above quantum chemistry calculation and experimental results fully confirmed our proposed reaction mechanism and verified the specific response of the fluorogenic probe to H_2S (Fig. 3f).

We are encouraged to use Mito-GW to image the distribution of mitochondrial H_2S in living cells due to the specificity and sensitivity of the fluorogenic in responding to H_2S. Firstly, we investigated the cell viability of Mito-GW on four cell lines to determine the working concentration of the probe used for bioimaging (Fig. S10 in Supporting information). We are excited that the viability of L02 cells remained above 95% when being treated with Mito-GW for 24 h. Therefore, 1 μmol/L Mito-GW would be used for the subsequent biological experiments unless otherwise indicated. Next, we exploited the subcellular localization of the probe in living cells. MitoTracker deep red (MitoTracker) was employed for the colocalization imaging with Mito-GW. As expected, the fluorescence imaging exhibited that there was a good overlap between MitoTracker (red channel) and Mito-GW (green channel) (Figs. S12 and S13 in Supporting information). This result demonstrates that the probe has specifically target mitochondria relying on the positive charge of the pyridine moiety. Then, L02 cells were incubated with Mito-GW at various times. The fluorescence intensities gradually increased overtime and reached its peak 3 h after incubation, indicating that the probe has a good response performance to H_2S in living cells (Fig. S14 in Supporting information).

Encouraged by the specific mitochondrial targeted and H_2S responsive abilities, we further employed Mito-GW to investigate the pattern of mitochondrial H_2S change in cellular hypoxia-reoxygenation processes. Hepatocyte hypoxia-reoxygenation system was developed to exhibit characteristics of liver ischemia/reperfusion injury as seen in humans and animal models (Figs. 4a, d, g). As shown in Figs. 4b, e, h), hypoxia conditions (3 h) led to an increasing of Mito-GW fluorescence signals as compared to levels of control group. However, a reoxygenation process declined the fluorescence signals that induced by hypoxia to a basal level. The above results indicated that Mito-GW can be used as an imaging tool to reveal the relationship between mitochondrial H_2S and hypoxia-reoxygenation.

We further examined the fluorogenic probe tracking of H_2S distribution and level fluctuations *in vivo* by establishing mice HIRI models (Figs. 5a and b). All experiments were conducted on male BALB/c mice (22–26 g). All the animal studies were performed following the guidelines for the Care and Use of Laboratory Animals of the Chinese Animal Welfare Committee and the protocol was approved by the Animal Health and Use Committee of Northwestern Polytechnical University. As shown in Figs. 5c and d, strong fluorescence was observed in ischemia group. Our experimental results were consistent with previous report that the lack of O_2 would block the activity of mitochondrial sulfide: quinone oxidoreductase (SQR) causes elevated levels of H_2S [20]. In contrast, the fluorescence signals of reperfusion tissues were significantly decreased compared to that of the ischemia group, implying that H_2S levels were suppressed after nutrition and oxygen restoration. These results demonstrated that Mito-GW could serve as a promising imaging tool for mapping fluctuation of H_2S under pathological conditions of liver ischemia/reperfusion.

In summary, we have fabricated a mitochondrial-targeted SMFP (Mito-GW) for detections of H_2S in HIRI sites. The probe exhibited a significant fluorescence emission at 602 nm with large Stokes shift (178 nm), and showed high specificity and sensitivity (LOD, 54 nmol/L) toward H_2S. The response mechanism of Mito-GW toward H_2S was confirmed *via* quantum chemistry calculation combined with HPLC experiments. Moreover, the fluorogenic probe was successfully used for monitoring mitochondrial H_2S-levels *in vitro* and *in vivo* HIRI models and performed well in indicating the changing tendency. We thus expect that our developed SMFP has the powerful potential for studying in hepatology to reveal the more details of HIRI. We also anticipate that the probe would be used to evaluate the drug efficacy of HIRI *in vivo*.

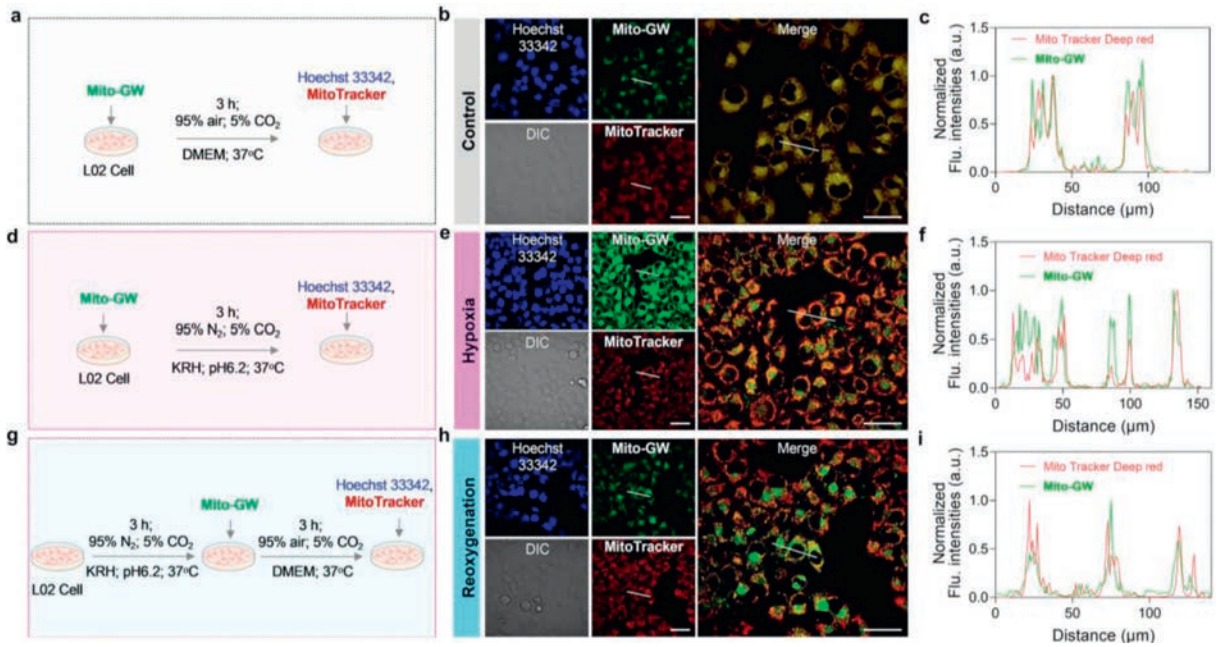

Fig. 4. Schematic illustration of the experimental protocol of control (a), hypoxia (d) and reoxygenation (g) groups. Fluorescence images of living L02 cells incubated with Mito-GW, MitoTracker deep red and Hoechst 33342 in control (b), hypoxia (e) and reoxygenation (h) groups. Images were collected from 560 nm to 620 nm for Mito-WG (λ_{ex} = 488 nm), 650–1000 nm for MitoTracker deep red (λ_{ex} = 640 nm), 400–450 nm for Hoechst 33342 (λ_{ex} = 405 nm). Scale bar: 40 μm. The normalized intensities profiles of regions of interest (ROIs) of Mito-WG and MitoTracker deep red in control group (c), hypoxia group (f) and reoxygenation group (i).

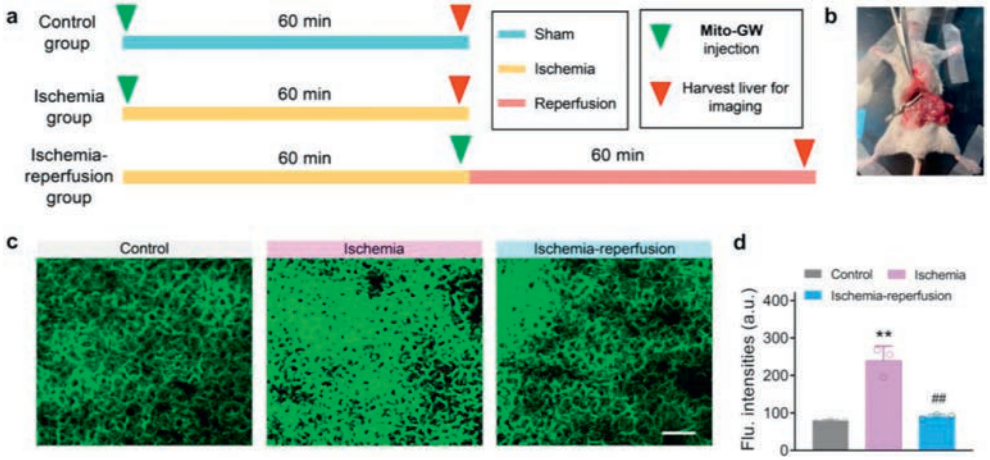

Fig. 5. (a) Schematic illustration of the experimental protocol of control, liver ischemia and ischemia-reperfusion group. (b) The hepatic ischemia-reperfusion mice model. (c) Representative fluorescence images of liver tissues in the three groups. Scale bar: 80 μm. (d) Average fluorescence intensities for c. Data were expressed as mean ± SD. $^{\#\#}P < 0.01$ *vs.* ischemia, $^{**}P < 0.01$ *vs.* control.

Declaration of competing interest

The authors declare that they have no known competing financial interests or personal relationships that could have appeared to influence the work reported in this paper.

Acknowledgments

This work was financially supported by the National Natural Science Foundation of China (Nos. 22077101, 22004099), the Joint Research Funds of Department of Science & Technology of Shaanxi Province and Northwestern Polytechnical University (Nos. 2020GXLH-Z-008, 2020GXLH-Z-021, 2020GXLH-Z-023), Natural Science Foundation of Shaanxi Province (No. 2022JM-130), The Natural Science Foundation of Ningbo (Nos. 202003N4049, 202003N4065), the Open Project Program of Wuhan National Laboratory for Optoelectronics (Nos. 2020WNLOKF023, 2022WNLOKF009), Innovation Foundation for Doctor Dissertation of Northwestern Polytechnical University (No. CX2022034). Innovation Capability Support Program of Shaanxi (No. 2023-CX-PT-23).

Supplementary materials

Supplementary material associated with this article can be found, in the online version, at doi:10.1016/j.cclet.2023.108913.

References

[1] J.H. Liu, W. Zhang, C.M. Zhou, et al., J. Am. Chem. Soc. 144 (2022) 13586.
[2] Y.D. Du, W.Y. Guo, C.H. Han, et al., Cell Death Dis. 12 (2021) 442.
[3] I. Jochmans, N. Meurisse, A. Neyrinck, et al., Liver Transpl. 3 (2017) 634–644.
[4] J.Y. Li, D.S. Yu, C.H. He, et al., Cell Death Dis. 14 (2023) 393.
[5] S. Monga, Nat. Med. 24 (2018) 6–7.
[6] B.L. Mao, W. Yuan, F. Wu, Y. Yan, B.L. Wang, Cell Death Discov. 9 (2023) 115.

[7] I. Andreadou, R. Schulz, A. Papapetropoulos, et al., J. Cell. Mol. Med. 24 (2020) 6510.
[8] Y.P. Zhang, X.R. Liu, M.W. Yang, S.L. Yang, F.F. Hong, World J. Hepatol. 14 (2022) 504.
[9] D.L. Ni, H. Wei, W.Y. Chen, et al., Adv. Mater. 31 (2019) 1902956.
[10] S.K. Chun, K. Go, M.J. Yang, et al., Toxicol. Res. 32 (2016) 35–46.
[11] M. Wang, J. Zhang, N. Gong, Ann. Palliat. Med. 11 (2022) 806–817.
[12] R.G. Bardallo, A.P. Roselló, S. Sanchez-Nuno, et al., FEBS J. 289 (2022) 5463.
[13] Y. Long, H. Wei, J. Li, et al., Nano Lett. 20 (2020) 6510.
[14] J. Mu, C. Li, Y. Shi, et al., Nat. Commun. 13 (2022) 2513.
[15] J. Xin, T. Yang, X. Wu, et al., Commun. Biol. 6 (2023) 194.
[16] S. Zhang, S. Rao, M. Yang, et al., Int. J. Mol. Sci. 23 (2022) 2357.
[17] X. Xu, G. Li, F. Zhang, G. Jiang, Z. Hao, Chin. Chem. Lett. 33 (2022) 1279–1282.
[18] Y. Zhang, J. Fang, S. Ye, et al., Nat. Commun. 13 (2022) 1685.
[19] X. Wu, Y. Lu, B. Liu, et al., Chin. Chem. Lett. 32 (2021) 2380–2384.
[20] B.D. Paul, S.H. Snyder, K. Kashfi, Redox. Biol. 38 (2021) 101772.
[21] A.K. Steiger, M. Marcatti, C. Szabo, et al., ACS Chem. Biol. 12 (2017) 2117.
[22] J.L. Miljkovic, N. Burger, J.M. Gawel, et al., Redox Biol. 55 (2022) 102429.
[23] S. Arndt, C.D. Baeza-Garza, A. Logan, et al., J. Biol. Chem. 292 (2017) 7761.
[24] K. Wang, Y. Du, Z. Zhang, et al., Nat. Biomed. Eng. 1 (2023) 161.
[25] B. Fang, Y. Shen, B. Peng, et al., Angew. Chem. Int. Ed. 134 (2022) e202207188.
[26] R. Chen, W. Li, R. Li, et al., Chin. Chem. Lett. 34 (2023) 107845.
[27] R. Zhai, B. Fang, Y. Lai, et al., Chem. Soc. Rev. 52 (2023) 942.
[28] J. Xing, Q. Gong, R. Zou, et al., Chin. Chem. Lett. 34 (2023) 107786.
[29] B. Fang, B.L. Zhang, R. Zhai, et al., New J. Chem. 46 (2022) 2487.
[30] X. Liu, Y.T. Chang, et al., Chem. Soc. Rev. 51 (2022) 1573.
[31] B. Fang, P.P. Li, J.M. Jiang, et al., Coord. Chem. Rev. 440 (2021) 213979.
[32] H. Fang, Y. Chen, Z. Jiang, et al., Acc. Chem. Res. 56 (2023) 258.
[33] J.Y. Guo, B. Fang, H. Bai, et al., Trends Anal. Chem. 155 (2022) 116697.
[34] L. Wu, J. Huang, K. Pu, T.D. James, Nat. Rev. Chem. 5 (2021) 406.
[35] H. Bai, B. Fang, X. Wang, et al., Chem. Commun. 57 (2021) 13186.
[36] Z. Fang, Z. Su, W. Qin, et al., Chin. Chem. Lett. 31 (2020) 2903–2908.
[37] X. Tian, T.Y. Liu, B. Fang, et al., ACS Appl. Mater. Interfaces 10 (2018) 31959.
[38] S.J. Li, Y.F. Li, H.W. Liu, et al., Anal. Chem. 90 (2018) 9418.
[39] T. Zhou, Y. Yang, K. Zhou, et al., Sens. Actuator. B: Chem. 301 (2019) 127116.
[40] Y. Zhang, W. Zhou, N. Xu, et al., Chin. Chem. Lett. 34 (2023) 107472.
[41] Y.M. Poronik, G.V. Baryshnikov, I. Deperasińska, et al., Commun. Chem. 3 (2020) 190.
[42] J. Miao, M.Q. Miao, Y. Jiang, et al., Angew. Chem. Int. Ed. 62 (2023) e202216351.